

Morphological analyses of $\text{Hg}_{1-x}\text{Ho}_x\text{Ba}_2\text{Ca}_2\text{Cu}_3\text{O}_{8+y}$ ($0.0 \leq x \leq 0.20$) superconductors fabricated by sol-gel technique

A. COŞKUN^{a,*}, A. EKICIBİL^b, H. ASLAN^c, S. K. ÇETİN^b, C. SARIKÜRKCÜ^d, K. KIYMAÇ^b

^a *Department of Physics, Faculty of Sciences and Letters, Mugla University, 48000, Mugla, Turkey*

^b *Department of Physics, Faculty of Sciences and Letters, Cukurova University, 01330 Adana, Turkey*

^c *Department of Physics, Faculty of Engineering and Natural Sciences, 34956, Istanbul, Turkey*

^d *Department of Chemistry, Faculty of Sciences and Letters, Mugla University, 48000, Mugla, Turkey*

This work reports a systematic study on the morphological properties of the superconducting compounds, $\text{Hg}_{1-x}\text{Ho}_x\text{Ba}_2\text{Ca}_2\text{Cu}_3\text{O}_{8+y}$ with $0.0 \leq x \leq 0.20$, prepared by using the so-called sol-gel method followed by a sealed quartz tube synthesis. The analyses of the synthesized products were performed by XRD, AFM, SEM and EDX methods. The results, obtained from the analyses of the XRD and EDX spectra or patterns, and the SEM and AFM images, indicate that the high- T_c Hg-(1223) and Hg-(1234) phases gradually disappear with increasing amounts of Ho. In addition it is observed that, Hg is excluded from the structure with the addition of Ho for Hg. As a result, it has been concluded that the high- T_c phases, Hg-(1223) and Hg-(1234), gradually disappear with increasing amount of Ho content, due to the exclusion of excess amount of Hg from the structures of the samples. This exclusion and observation may be attributed either to the quite different sizes of Ho and Hg ions or to the large HgO powders compared to the sol-gel powders and/or even to the sample preparation method used in this work.

(Received April 12, 2010; accepted November 10, 2010)

Keywords: Atomic force microscopy, Characterization, X-ray diffraction, Oxide superconducting materials

1. Introduction

Hg-based superconductors, $\text{HgBa}_2\text{Ca}_{n-1}\text{Cu}_n\text{O}_{2n+2+\delta}$ ($n=1,2,3\dots$), are of great interest; since high critical temperatures T_c [1-7] were reported as $T_c=133\text{K}$ for Hg-(1223) [1], $T_c=94\text{K}$ for Hg-(1202) [2], $T_c=121\text{K}$ for Hg-(1212) [6] and $T_c=126\text{K}$ for Hg-(1234) [7]. These Hg-cuprates, however, show very weak pinning behavior. Although these specialties make Hg series attractive to study, because of the difficulties in processing and toxic effects, researchers are in general unwilling to prepare them. There are several ways to prepare a Hg-based cuprate superconductor: The most common ways are the sealed silica tube or high pressure techniques. These compounds are found to have very short coherence lengths. One of the implications of the extremely short coherence length in cuprates, typically a few angstroms, is that superconducting properties, especially, critical current densities of these materials are sensitive to their underlying microstructure. However, for instance, a significant improvement in superconducting properties of both, bulk and film forms of the Y and Bi-based superconductors have been obtained by several workers through understanding and control of their microstructural characteristics [8-16]. The same approaches can be applied to the Hg-based superconductors.

The Hg-based (1212)-type superconducting compound was first identified in the HgBaRECuO (RE=rare earths) system by Putilin et al. [17] and in the HgTlSrCaYCuO system by Liv et al. [18]. The Hg-(1212) type phase has the following features; its crystal structure

is similar to that of the (1234)-phase; it can be widely subjected to elemental substitutions (for example, Tl, Pb, Bi, Re, Mo, Ho, Cr, etc.) for obtaining new materials; the T_c of this family varies from 65 to 128K and strongly depend on the species of substitutes [18-22]. In this work, our aim is to explore the effects of Ho replacement for Hg on the superconductivity of the compounds, HgBaCaCuO , by using X-ray diffraction (XRD), scanning electron microscopy (SEM), X-ray energy dispersive spectroscopy (EDX), and atomic force microscopy (AFM) measurements. Samples were prepared with sol-gel method, which is one of the most reliable methods for obtaining a super homogenization of the elements at an atomic scale, followed by a solid state reaction technique.

2. Experimental procedure

In this study, first the $\text{Ho}_x\text{Ba}_2\text{Ca}_2\text{Cu}_3\text{O}_{8+y}$ compounds where ($x=0.00, 0.05, 0.10, 0.15, 0.20$), have been prepared by sol-gel method as follows: Appropriate amounts of Ho_2O_3 , BaCO_3 , CaCO_3 and CuO with desired stoichiometries were dissolved in dilute HNO_3 solution at $150\text{ }^\circ\text{C}$. Then citric acid and ethylene glycol were added to the mixture. Viscous residual was formed by slowly boiling this solution at $200\text{ }^\circ\text{C}$. The obtained residual was then dried slowly at $300\text{ }^\circ\text{C}$ until a dry-gel was formed. Finally, the residual precursor was burned in air at $600\text{ }^\circ\text{C}$ in order to remove organic materials produced during chemical reactions. Then the resulting nano powders of $\text{Ho}_x\text{Ba}_2\text{Ca}_2\text{Cu}_3\text{O}_{8+y}$ and HgO powder were mixed in different ratios and were homogenized in an agat mortar

and pressed to form pellets. The pellets were sealed in quartz tubes which were then sintered at 850 °C for 10 h and slowly cooled to room temperature. The samples so obtained have the compositions of $\text{Hg}_{1-x}\text{Ho}_x\text{Ba}_2\text{Ca}_2\text{Cu}_3\text{O}_{8+y}$ with $x=0.00, 0.05, 0.10, 0.15, 0.20$, and are labeled as A, B, C, D and E respectively. The structural analyses of the samples were then carried out with XRD, AFM, SEM and EDX.

3. Results and discussions

As stated above, the samples with nominal compositions of $\text{Hg}_{1-x}\text{Ho}_x\text{Ba}_2\text{Ca}_2\text{Cu}_3\text{O}_{8+y}$, $0.00 \leq x \leq 0.20$, were prepared and the effects of Ho substitution for Hg were analyzed morphologically by using XRD, AFM, SEM and EDX. The XRD pattern of the samples are shown in Fig. 1. The XRD data collected from various samples show that all the samples indicate polycrystalline, complex and disoriented crystal formations having tetragonal Hg-(1234), Hg-(1223) and Hg-(1212) superconducting phases. For $x=0.00$, traces of CaHgO_2 are also observed. The XRD patterns show also some impurity and unknown phases for small concentrations of Ho. However, for $x \geq 0.10$, unknown phases are appeared in all of the concentrations, whose amount increases with increasing Ho content. The main XRD peak of these unknown phases is somewhere in between 30-34° and its proportion increases with the Ho content.

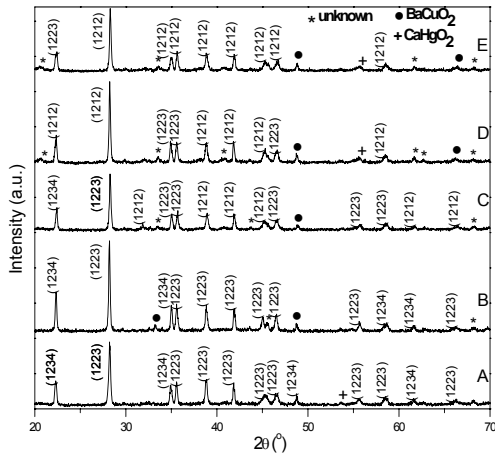


Fig. 1. XRD patterns of $\text{Hg}_{1-x}\text{Ho}_x\text{Ba}_2\text{Ca}_2\text{Cu}_3\text{O}_{8+y}$; A) $x=0.00$, B) $x=0.05$, C) $x=0.10$, D) $x=0.15$, E) $x=0.20$.

The structural and superconducting parameters for the $\text{Hg}_{1-x}\text{Ho}_x\text{Ba}_2\text{Ca}_2\text{Cu}_3\text{O}_{8+y}$ series are summarized in Table 1. The lattice parameters were calculated from the XRD spectra by considering the $p4/mmm$ space group symmetry in the tetragonal form. We can say that the XRD patterns for Ho doped samples resemble each other except for some changes in unit cell dimensions. They decrease with increasing Ho content. In other words, the increase in the Ho concentration has caused a slight decrease in the a -parameter whereas a pronounced decrease in the c -parameter, as shown in Fig. 2, in agreement with previously reported results [2-5,18,19]. The pronounced variations in the c -parameter of the samples can be explained to be due to the ionic radius of Ho (2.47 Å) being larger than that of Hg (1.76 Å). Fig. 3 shows the variations of the unit cell volume and the volume fractions of the high temperature superconductor phase (HTSC) as a function of x . The volume fractions of the HTSC phase, Hg-(1223), of the samples, $0.0 \leq x \leq 0.20$, are about 69, 66, 50, 30 and 11 % for the samples A, B, C, D and E, respectively. The samples A and B also contain about 30 and 33 % Hg-(1234) phase, respectively. In another words, the samples A and B have higher volume fractions of the Hg-(1223) and Hg-(1234) phases than those of the samples C, D and E, indicating that the formations of Hg-(1223) and Hg-(1234) phases are reduced by Ho doping. Hg-(1223) and Hg-(1234) are the main phases for the samples A and B. Fig. 4 shows the variations of the maximum intensity I_{max} of the Hg-(1223), Hg-(1234) and Hg-(1212) phases against x concentrations. It is observed that I_{max} of Hg-(1223) and Hg-(1234) phases decrease with increasing Ho content, and vice versa for the Hg-(1212) phase. This means that the substitution of Ho, with higher ionic size, for Hg decreases the intergranular contacts and leads to the inadequate formation of the Hg-(1223) and Hg-(1234) phases in our samples. This later observation related to I_{max} is in agreement with the trend of volume fractions of the Hg-(1223) phase.

Table 1. Nominal composition and structural parameters of $\text{Hg}_{1-x}\text{Ho}_x\text{Ba}_2\text{Ca}_2\text{Cu}_3\text{O}_{8+y}$.

Samp.	Ho content, x	Main phases	Lattice parameters for the main HTSC phases		Unit cell volume, (Å ³)	Volume fraction of HTSC phases (%)		Symmetry	I_{max} (1212) (a.u.)	I_{max} (1223) (a.u.)	I_{max} (1234) (a.u.)
			a (Å)	c (Å)		(1223)	(1234)				
A	0.00	(1223),(1234)	3.809(9)	12.851(5)	187.524	69	30	Tetragonal	-	1100	500
B	0.05	(1223),(1234)	3.807(6)	12.001(3)	173.992	66	33	Tetragonal	-	900	400
C	0.10	(1212),(1223)	3.806(6)	11.952(1)	173.279	50	-	Tetragonal	350	830	370
D	0.15	(1212)	3.804(4)	11.121(4)	160.965	30	-	Tetragonal	420	490	-
E	0.20	(1212)	3.801(3)	11.002(3)	158.981	11	-	Tetragonal	910	310	-

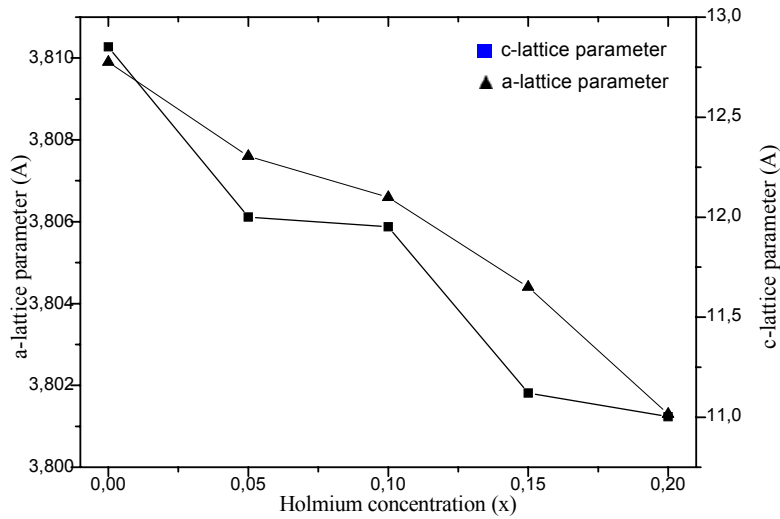


Fig. 2. Lattice parameters of superconducting $Hg_{1-x}Ho_xBa_2Ca_2Cu_3O_{8+y}$ as a function of Ho-content, x .

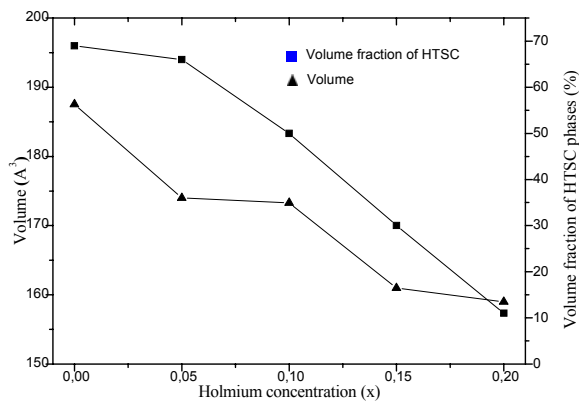


Fig. 3. Variation of volume fractions of the HTSC phase, Hg-(1223), and unit cell volume as a function of Ho-content, x .

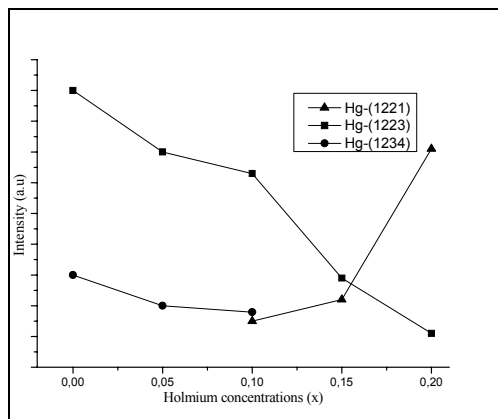


Fig. 4. Intensity of Hg-(1223), Hg-(1234) and Hg-(1212) superconducting phases versus Ho concentrations for $Hg_{1-x}Ho_xBa_2Ca_2Cu_3O_{8+y}$.

The surface morphologies of the mercury-based holmium doped superconducting compounds were investigated by AFM, SEM and EDX. The Atomic Force Microscopy (AFM) images of the samples were taken via contact mod with $5 \mu\text{m} \times 5 \mu\text{m}$ in size, and are given in Fig. 5. A granular structuring in sample A, which is free of Holmium doping, is eye catching. Grains, which are getting together and about to join one another, are observed on the surface of this sample. Average grain sizes vary between 0 and $0.5 \mu\text{m}$. It is not possible to say that a complete granular structuring has taken place, since the grains seem to have formed random clumps. The loosely packed surface morphology of this sample indicates the fact that the heat treatment temperature and time were not probably sufficient. Holmium ions that enter the structure make the surface morphology of the holmium doped samples different from that of the undoped sample. However, the growth of grains in clumps that took place on the surfaces of the holmium free sample has to some extent also taken place on the surfaces of the doped samples. In addition, grains that constitute these clumps are smaller and clumps are more separated from each other. It seems that the grain sizes have remained the same and grains have got intertwined as a result of disintegration of the clumped structure. These samples have also porosity. In addition, the surface of the samples with $x=0.10$, 0.15 and 0.20 (samples B, C and D) have some small particles. These small particles seem to have formed as a result of more holmium ions entering in to the clumped structure. Furthermore, the sizes of the particles have become smaller with increasing holmium concentration. We believe that these behaviors stem from the disintegration of the clumped structure.

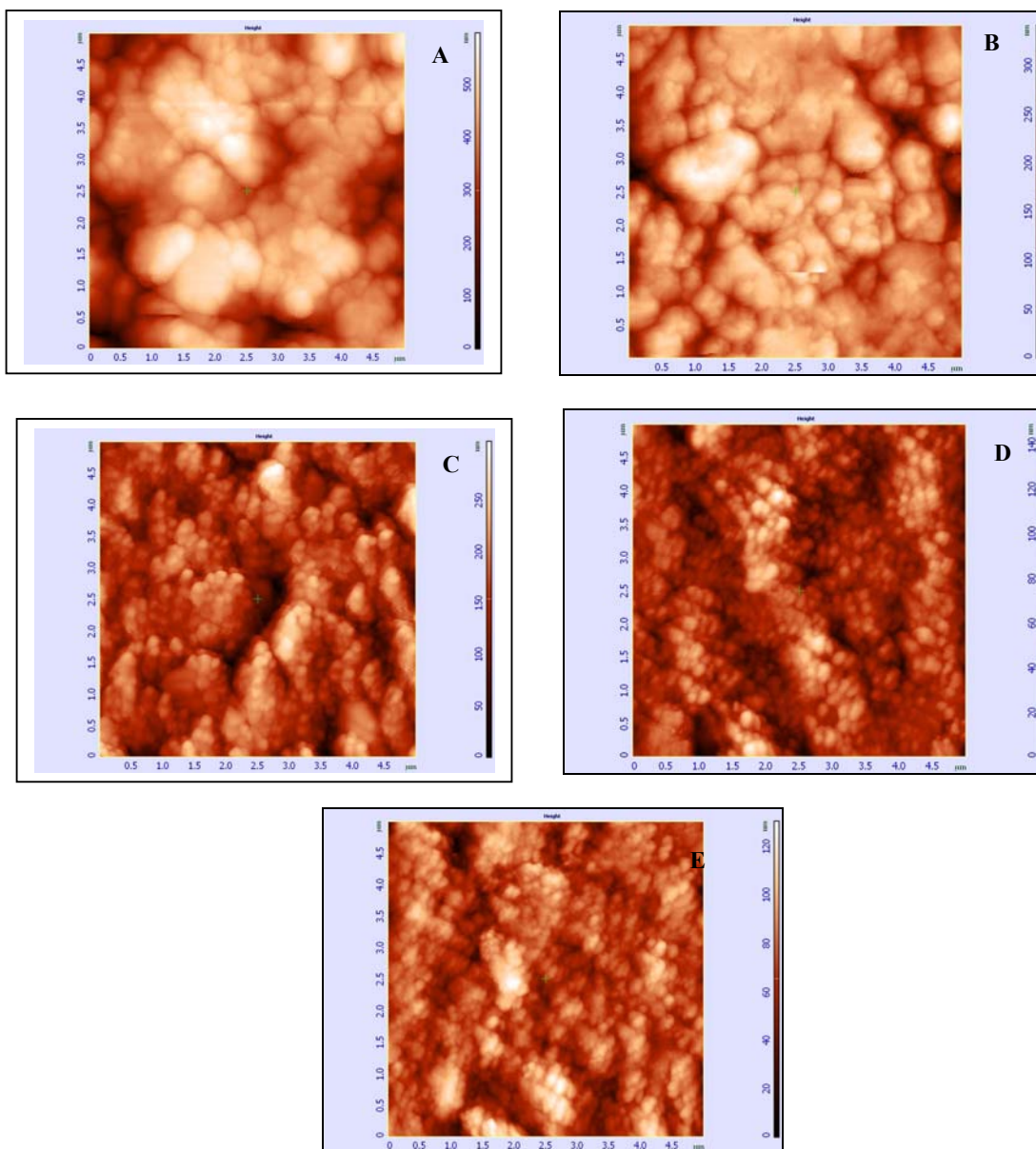


Fig. 5. AFM images of precursor materials $\text{Hg}_{1-x}\text{Ho}_x\text{Ba}_2\text{Ca}_2\text{Cu}_3\text{O}_{8+y}$; A) $x=0.00$, B) $x=0.05$, C) $x=0.10$, D) $x=0.15$, E) $x=0.20$.

The SEM images of the sample's surfaces shown in Fig. 6 are 2500 times magnified. It is quite clear that the surface morphology of the holmium free sample is quite different from those of the others, in agreements with the AFM images. Two distinct formations on the surface of this sample are remarkable. One of them is the main structure covering the surface of the sample, and the other is the randomly distributed plate-like formations. These formations were proved to be pure mercury particles by EDX analysis, as shown in Fig. 7 and especially in Fig. 8.

There are two reasonable explanations for this kind of formation to occur, in this study. Firstly, HgO powders used during the preparation of the compounds were added to HfBaCaCuO powders, after the sol-gel processing of the later, and the resulting powders were homogenized in an agate mortar. This method may have led to an accumulation of micron sized HgO powders in the samples. Secondly, the selected heat treatment temperature might not be appropriate for the purpose. As it is well known, HgO decomposes as Hg and O at relatively low

temperatures. If the sizes of mercury particles are larger than the grains of the main structure, it is expected that the metallic mercury spreads over the surface instead of being placed at the grain boundaries of the structure. This argument is supported by the observation that during the preparation of the sample some metallic Hg was seen, after sintering process, over the inner surface of the quartz crucibles in which the samples were placed for sintering. This situation has arisen from the chosen method for the

production of the Hg-based superconductors. When preparing a Hg-based superconducting material, keeping Hg in compound material is the greatest problem. If that is accomplished, superior superconducting properties may be achieved. In this study, we had some how difficulties in achieving the mentioned objective, probably due to the chosen method.

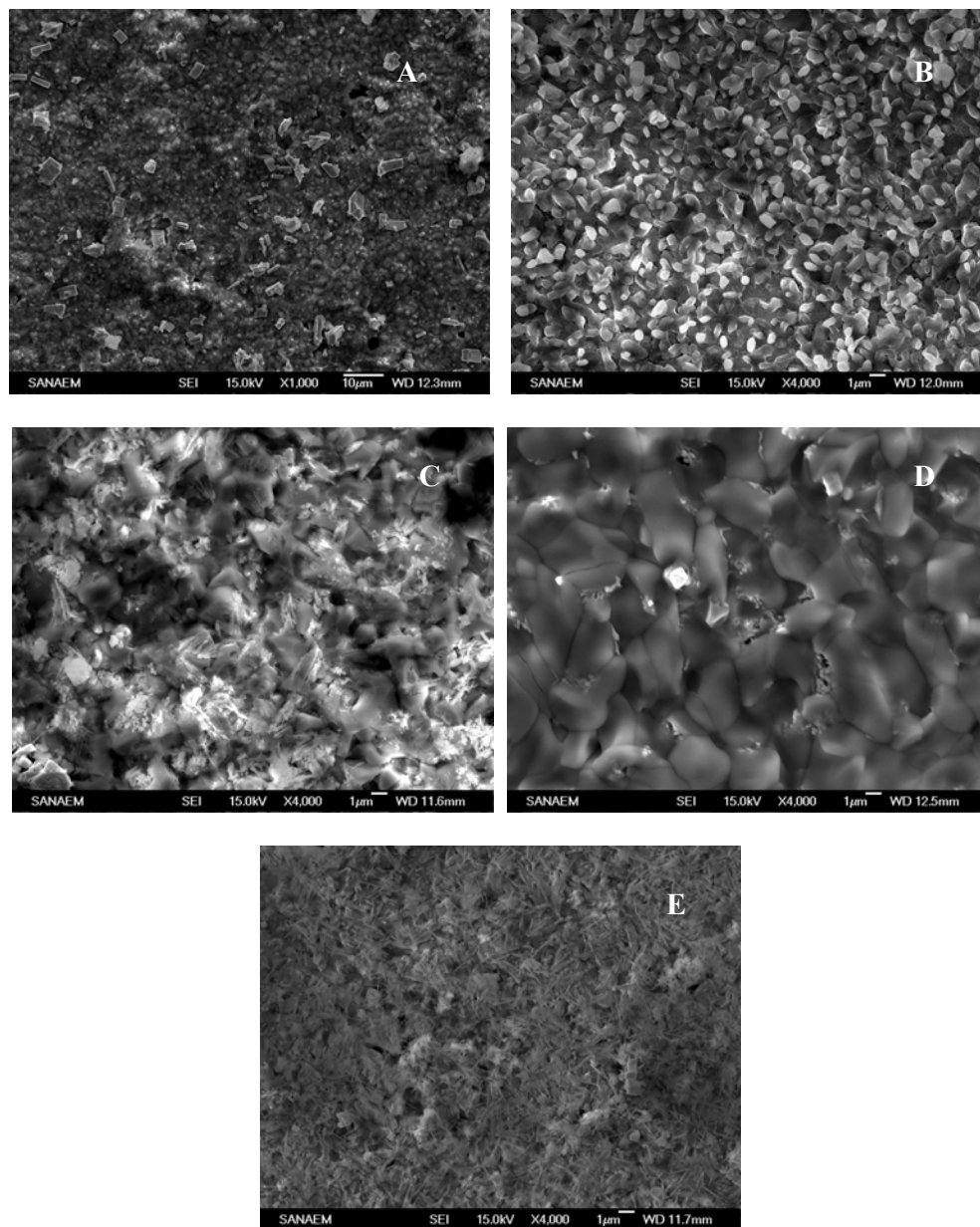


Fig. 6. SEM images of $Hg_{1-x}Ho_xBa_2Ca_2Cu_3O_{8+y}$; A) $x=0.00$, B) $x=0.05$, C) $x=0.10$, D) $x=0.15$, E) $x=0.20$.

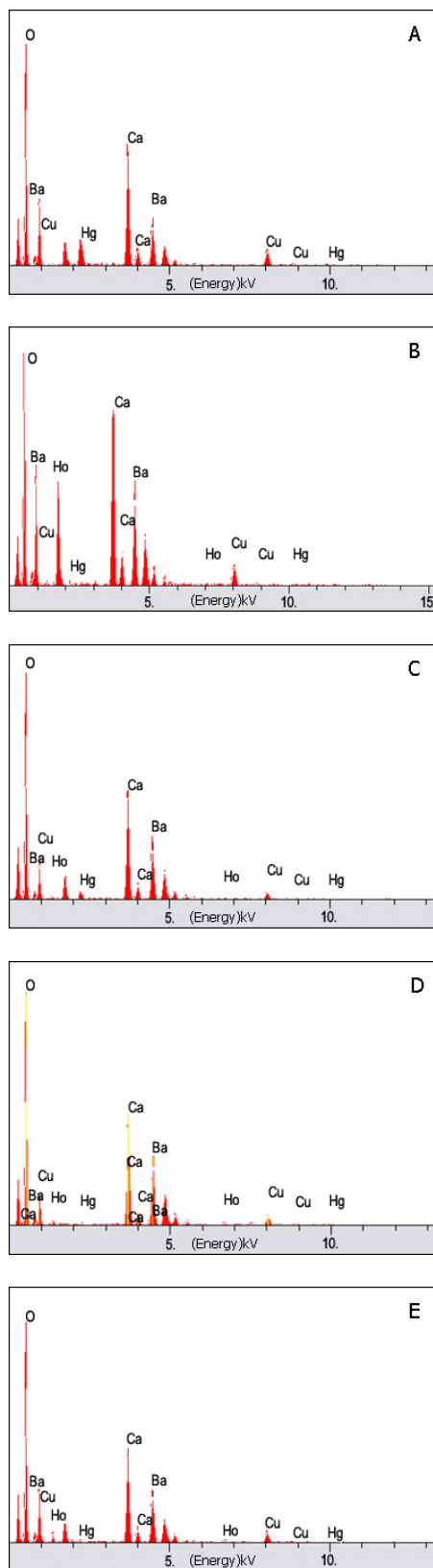


Fig. 7. EDX spectra of $\text{Hg}_{1-x}\text{Ho}_x\text{Ba}_2\text{Ca}_2\text{Cu}_3\text{O}_{8+y}$, indicating the presence of different elements. A) $x=0.00$, B) $x=0.05$, C) $x=0.10$, D) $x=0.15$, E) $x=0.20$.

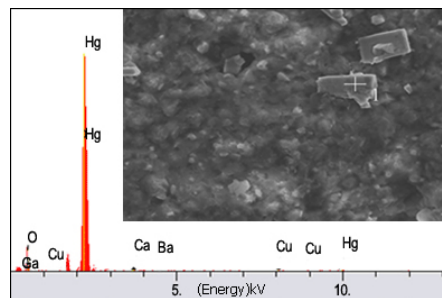


Fig. 8. Point analysis of EDX spectra of $\text{Hg}_{1-x}\text{Ho}_x\text{Ba}_2\text{Ca}_2\text{Cu}_3\text{O}_{8+y}$ indicating the presence of Hg at the marked plate (area).

The surface morphology of the samples changes as a consequence of holmium diffusion into the structure. The SEM images indicate that Ho concentration is effective on the structure of the samples; i.e., increased amount of Ho ions causes an unusual decrease or increase in the grain sizes. However, these unusual SEM images might also be affected from the improbable duration of the thermal processes and the incorrect setting of the sintering temperatures by which we hoped to obtain good crystallized superconducting samples. The grains on the surface of $x=0.05$ holmium doped sample are more pronounced. Metallic Hg is also seen over the surface of this sample through a low magnified SEM image. The average grain size of this sample is smaller than $1 \mu\text{m}$. A partial melting has occurred over the surface of the 0.10 holmium doped sample. Small sized, randomly oriented bar shaped formations are observed in the regions between the grains of this sample. This situation may stem from inappropriately chosen heat treatment duration and/or sintering temperature. The surface of the 0.15 holmium doped sample consists of tightly connected, well grown grains of 3 to $4 \mu\text{m}$ in size. The formations seen between the grains of the 0.10 holmium doped sample, have arisen on this sample as well. However, the surface of this highly doped sample seems to be quite different from that of the others. A bar shaped structuring, rather than the granular structuring, is prominent on the surface of this sample i.e., the bar shaped structures, existing at the grain boundaries of the previous samples, appear to spread over the whole structure of this sample. Randomly distributed metallic mercury particles have been observed again on a low magnified SEM image as observed on the former samples.

Consequently, from the AFM and the SEM images and the XRD and EDX analyses it has been concluded that the changes take place negatively as a result of introducing holmium in to the structure, i.e., high temperature phases, Hg-(1223) and Hg-(1234), have gradually disappeared with increasing Ho content. Besides, mercury exclusion from the main structure has been found by using EDX analysis. Thus it has been concluded that either the technique utilized in this work for preparing the Hg-based superconductors, that we aimed at, is not suitable or the sizes of HgO powder were quite larger than the sol-gel powder. In this sense, if at the beginning HgO powders with nanometer size were used to mix with the powders

obtained from the sol-gel, reaching at a better result would have been possible.

4. Conclusions

In this study, we have synthesized the $\text{Hg}_{1-x}\text{Ho}_x\text{Ba}_2\text{Ca}_2\text{Cu}_3\text{O}_{8+y}$ superconducting compounds, with $0.00 \leq x \leq 0.20$. We have investigated the effects of substitution of Holmium ions for Hg ions with emphasis on correlation between superconducting properties and morphological features. The morphology of grains shows clear and distinct changes with increasing Ho content. The changes of the morphological features and superconducting properties may be due to the chemical as well as the electronically inhomogeneities in the structures. The AFM and SEM analyses demonstrate that precursor materials prepared by sol-gel method have nanosized particles as shown in Figs. 5 and 6. By comparing the particle sizes we can clearly see the effects of concentration, that is, the particle sizes decrease with increasing Ho concentration. The stoichiometry corresponding to various compositions were verified by XRD and EDX, which reveal that the estimated stoichiometries are found to be in conformity with the envisaged stoichiometries. EDX shows that the unknown phases appearing in EDX spectra (Fig. 7) may be mainly Ho. They could also incorporate Cu or Ca in few amounts but the conclusion on this point is not definite. In addition, Fig. 8 that shows the point analysis of the EDX spectra of $\text{Hg}_{1-x}\text{Ho}_x\text{Ba}_2\text{Ca}_2\text{Cu}_3\text{O}_{8+y}$, in order to explore the elements at a definite point (such as marked on the figure), and indicates that Hg is located at the marked area. We have concluded that the microstructural developments of Hg-(1223) and Hg-(1234) superconductors quite depend on heat treatments and control of Hg and O_2 vapor pressures during syntheses. In our study, Hg-(1223) and Hg-(1234) phases have gradually disappeared with increasing Ho content, indicating that an excess amount of Hg was excluded from the structure.

Acknowledgements

We wish to thank Mustafa Akyol and Aydin Eraydin for their help.

References

- [1] A. Schilling, M. Cantoni, J. D. Guo, H. R. Ott, *Nature* **363**, 56 (1993).
- [2] S. N. Putilin, E. V. Antipov, O. Chmaissem, M. Marezio, *Nature* **362**, 226 (1993).
- [3] R. L. Meng, L. Beauvais, X. N. Zhang, Z. J. Huang, Y. Y. Sun, Y. Y. Xue, C. W. Chu, *Physica C* **216**, 21 (1993).
- [4] S. M. Loureiro, E. V. Antipov, J. L. Tholence, J. J. Capponi, O. Chmaissem, Q. Huang, M. Marezio, *Physica C* **217**, 253 (1993).
- [5] S. Tautkus, R. Kazlauskas, A. Kareiva *Talanta* **52**, 189 (2000).
- [6] S. N. Putilin, E. V. Antipov, M. Marezio, *Physica C* **212**, 266 (1993).
- [7] E. V. Antipov, S. M. Loureiro, C. Chaillout, J. J. Capponi, P. Bordet, J. L. Tholence, S. N. Putilin, M. Marezio, *Physica C* **215**, 1 (1993).
- [8] C. T. Lin, *Physica C* **337**, 312 (2000).
- [9] H. J. Scheel, P. Niedermann, *J. Cryst. Growth* **94**, 281 (1989).
- [10] P. G. Barbar, J. J. Pretty, *J. Cryst. Growth* **112**, 613 (1991).
- [11] A. Schilling, R. Jin, H. R. Ott, Th. Wolf, *Physica C* **235-240**, 2741 (1994).
- [12] G. Calestani, M. G. Francesconi, G. Salsi, G. D. Andreotti, A. Migliori, *Physica C* **197**, 283 (1992).
- [13] H. U. Krebs, Ch. Krauns, X. Yang, V. Geyer, *Appl. Phys. Lett.* **59**(17), 2180 (1991).
- [14] M. Hindow, M. Yeadon, *Philos. Mag. Lett.* **70** (1), 47 (1994).
- [15] R. Sun, H. P. Lang, H. J. Guntherodt, *Appl. Surf. Sci.* **86**, 140 (1995).
- [16] B. Dam, J. H. Rector, J. M. Huijbregtse, R. Griessan, *Physica C* **296**, 179 (1998).
- [17] S. N. Putilin, I. Bryntse, E. V. Antipov, *Mater. Res. Bull.* **26**, 1299 (1991).
- [18] R. S. Liv, S. F. Hu, D. A. Jefferson, P. P. Edwards, P. D. Hunneyball, *Physica C* **205**, 206 (1993).
- [19] E. Kandyel, *J. Physics and Chemistry of Solids* **64**, 731 (2003).
- [20] A. Schilling, M. Cantoni, J. D. Guo, H. R. Ott, *Nature(London)* **363**, 56 (1993).
- [21] O. Chmaissem, Z. Z. Sheng, *Physica C* **242**, 32 (1992).
- [22] E. Kandyel, X. J. Wu, S. Adachi, S. Tajima, *Physica C* **322**, 9 (1999).

*Corresponding author: coskunatilla@gmail.com